MOLECULAR ONCOLOGY 1 (2008) 431–439

available at www.sciencedirect.com

ScienceDirect

www.elsevier.com/locate/molonc

The apoptosis linked gene ALG-2 is dysregulated in tumors of various origin and contributes to cancer cell viability

Jonas M. la Cour[a], *Berit R. Høj*[a], *Jens Mollerup*[a], *Ronald Simon*[b], *Guido Sauter*[b], *Martin W. Berchtold*[a,*]

[a]*Copenhagen Biocenter, Department of Molecular Biology, University of Copenhagen, Ole Maaløes Vej 5, 2200 Copenhagen N, Denmark*
[b]*Department of Pathology, University Medical Center Hamburg-Eppendorf, Hamburg, Germany*

ARTICLE INFO

Article history:
Received 26 June 2007
Received in revised form
14 August 2007
Accepted 14 August 2007
Available online 19 August 2007

Keywords:
Calcium binding proteins
Tissue microarray
Gene silencing
ALG-2

ABSTRACT

The apoptosis linked gene-2 (ALG-2), discovered as a proapoptotic calcium binding protein, has recently been found upregulated in lung cancer tissue indicating that this protein may play a role in the pathology of cancer cells and/or may be a tumor marker. Using immunohistochemistry on tissue microarrays we analysed the expression of ALG-2 in 7371 tumor tissue samples of various origin as well as in 749 normal tissue samples. Most notably, ALG-2 was upregulated in mesenchymal tumors. No correlation was found between ALG-2 staining intensity and survival of patients with lung, breast or colon cancer. siRNA mediated ALG-2 downregulation led to a significant reduction in viability of HeLa cells indicating that ALG-2 may contribute to tumor development and expansion.

1. Introduction

ALG-2 (apoptosis linked gene-2) was discovered in a genetic screen and proposed to have a proapoptotic function as antisense ALG-2 RNA inhibited apoptosis induced by T-cell cross-linking in a T-cell hybridoma cell line (Vito et al., 1996). Sequence comparison and direct binding experiments indicated that ALG-2 is a Ca^{2+} binding protein of the EF-hand type belonging to the subfamily of PEF proteins (Maki et al., 1997). The best-characterized target of ALG-2 is AIP1/Alix, an adaptor protein, which has been shown to bind to many growth-related signaling proteins (reviewed in (Odorizzi, 2006)). Recently, it was found that AIP1/Alix plays a role in endocytosis related processes including virus budding (Strack et al., 2003; von Schwedler et al., 2003) and multivesicular endosome formation (Matsuo et al., 2004). AIP1/Alix induces apoptosis and reduces tumorigenicity in several cell lines (Chatellard-Causse et al., 2002; Wu et al., 2002). In addition, AIP1/Alix overexpression in chick embryos led to ALG-2 dependent apoptosis (Mahul-Mellier et al., 2006). Yet, overexpression of AIP1/Alix inhibited an alternative cell death program, named paraptosis (Sperandio et al., 2004). Recently, we (la Cour et al., 2007) and others (Shibata et al., 2007; Yamasaki et al., 2006) found that ALG interacts with Sec31A, a component of the COPII complex involved in

* *Corresponding author*. Tel.: +45 35322089; fax: +45 35322128.
E-mail address: mabe@my.molbio.ku.dk (M.W. Berchtold).

Abbreviations: ALG-2, apoptosis linked gene-2; TMA, tissue microarray; MTA, multitumor array; NTA, normal tissue array; PEF, penta EF-hand proteins; SDS, sodium dodecyl sulfate; DTT, dithiothreitol; SDS-PAGE, SDS-polyacrylamide gel electrophoresis; PVDF, polyvinyl difluoride; GIST, gastrointestinal tumors; DCIS, ductal carcinomas in situ; PNET, pancreatic neuroendocrine tumor; 7AAD, 7-amino-actinomycin D; SEM, standard error of the mean.

1574-7891/$ – see front matter
doi:10.1016/j.molonc.2007.08.002

trafficking proteins from the ER to the Golgi apparatus. ALG-2 interacts with Sec31A in a Ca^{2+}-dependent way and regulates its subcellular localization (Yamasaki et al., 2006).

ALG-2 is expressed in all so far analysed tissues and cell lines as shown by transcript analyses (Tarabykina et al., 2000; Vito et al., 1996) as well as by Western blot analyses (la Cour et al., 2003). Initial studies on ALG-2 localization in tumors have to be questioned due to the lack of specificity of the used antibody (Mollerup et al., 2003). We have recently generated a polyclonal antibody against ALG-2 and proven its specificity by preabsorption experiments as well as by testing it in a cell line where the ALG-2 gene was knocked out (la Cour et al., 2003). Using this antibody we showed that ALG-2 is upregulated in a rat hepatoma and in several human lung tumors. Staining intensities were up to 43% higher in small cell lung carcinomas as compared to corresponding normal lung tissue and also large cell lung carcinomas, lung adenocarcinomas and squamous carcinomas of the lung showed significantly higher ALG-2 expression. Moderate staining was found in type II pneumocytes, macrophages and epithelial cells of the bronchiae and alveoli in normal tissue, and strong staining was observed in most cancer cells (la Cour et al., 2003). Based on these results, we asked whether ALG-2 is generally upregulated in tumors. If this was the case it would be of interest to establish whether ALG-2 expression in tumors could have a prognostic value and whether ALG-2 potentially contributes to the transformed cellular phenotype. The previously reported high expression of ALG-2 in some cancers could indicate that ALG-2 plays a role in abnormal cell growth. Therefore, we analysed the effect of ALG-2 knockdown on HeLa cell growth and viability.

The tissue microarray (TMA) technique enables simultaneous expression analysis in thousands of tissue samples with an unprecedented degree of standardization. It allows for rapid and comprehensive analyses of virtually all types of human tumor, and facilitates powerful statistical analyses to search for associations between molecular markers and clinico-histological parameters (Kononen et al., 1998). In addition, the tissue architecture is fully preserved, allowing for detailed analysis even of normal tissues that are composed of various cell types. With the present study we have extended our initial analysis (la Cour et al., 2003) with 8120 neoplastic and normal tissues. Furthermore, we have evaluated the potential of ALG-2 as a prognostic marker and investigated the phenotype of a cancer cell line after downregulation of ALG-2. Besides providing a catalogue of ALG-2 expression we show that ALG-2 is highly expressed in several different cancer types and that ALG-2 knockdown results in a severe growth inhibition. This finding challenges the view of ALG-2 being a positive player in apoptotic pathways.

2. Results

2.1. Tumor types with ALG-2 expression

3191 tumor samples of 128 tumor types were analysed for ALG-2 staining intensity using the multitumor array (MTA) (Supplementary Table ST1). Of the 128 individual tumor types sorted according to a weighted staining intensity Brenner tumor of the ovary topped the ranking list followed by carcinoid tumor, cribriform breast cancer, pancreatic neuroendocrine tumors (PNET) and serous cancer of the ovaries (Figure 1, Table 1). Ranking the 19 tumor groups according to moderate and strong staining intensity yielded a list topped by tissue from non-invasive urinary bladder cancer (Table 2), whereas malignant urothelium was ranked 12th. No correlation was found between the ALG-2 levels and tumor stage progression as ALG-2 levels in neoplastic colon tissue from mild dysplasia over moderate dysplasia to severe dysplasia adenoma and finally colon adenocarcinoma decreased. Only 8% of benign mesenchymal tumors showed detectable ALG-2 staining, whereas 51% of sarcomas stained positive for ALG-2 (Table 2). Remarkably, no ALG-2 staining was found in muscle or skin tissue, whereas leiomyosarcomas and synovial sarcomas exhibited moderate/strong ALG-2 staining as did malignant melanomas and benign tumors of the appendix (Supplementary Table ST1, Figure 1). Gastrointestinal tumors (GIST) were found to be the most strongly stained sarcoma type with 77.5% of the samples stained and ranking 10th of all individual tumor types in weighted staining intensity (Figure 1, Table 1).

2.2. ALG-2 expression in cancers of the breast, colon, and lung

To explore the relationship between ALG-2 expression and clinico-pathological parameters in prevalent human cancer types, tumor type specific TMAs of breast, colon, and lung cancers were analysed. Almost all normal, benign or premalignant breast tissues showed weak to moderate expression of ALG-2. Lack of expression was only seen in 4.6% of normal breast samples and 4% of ductal carcinomas in situ (DCIS). In contrast, cancers showed more frequently loss of expression (10–30%) but also strong staining in rare cases ($\leq$15%). Strong expression was slightly more frequent in papillary (15%; $p = 0.33$) and mucinous cancers (10%; $p = 0.15$) as compared to ductal carcinoma (7.1%). Overall, ALG-2 expression was linked to high grade ($p = 0.0135$) and metastatic disease ($p = 0.0335$), but, unrelated to tumor stage ($p = 0.09$). Weak to moderate ALG-2 expression was found in about two-thirds of colon cancers irrespective of the histological subtype. Strong staining was rare (8.2–8.5% in adenocarcinoma and mucinous colon cancer). ALG-2 positivity was unrelated to pathological parameters including tumor stage, grade, and nodal stage. As compared to breast or colon cancer, ALG-2 staining was more frequently found to be intense in lung cancers. For example, 19.9% of adenocarcinomas and 26.9% of bronchioalveolar cancers showed strong ALG-2 expression. ALG-2 staining in malignant lung tissue was, however, unrelated to tumor stage, histological grade, or presence of lymph node or distant metastases. ALG-2 levels were unrelated to patient survival in breast ($p = 0.4445$), colon ($p = 0.5234$), and lung cancers ($p = 0.2040$; Figure 2).

2.3. ALG-2 expression in normal tissue

Data on ALG-2 expression in normal tissue were derived both from the staining of ALG-2 of the normal tissue array (NTA)

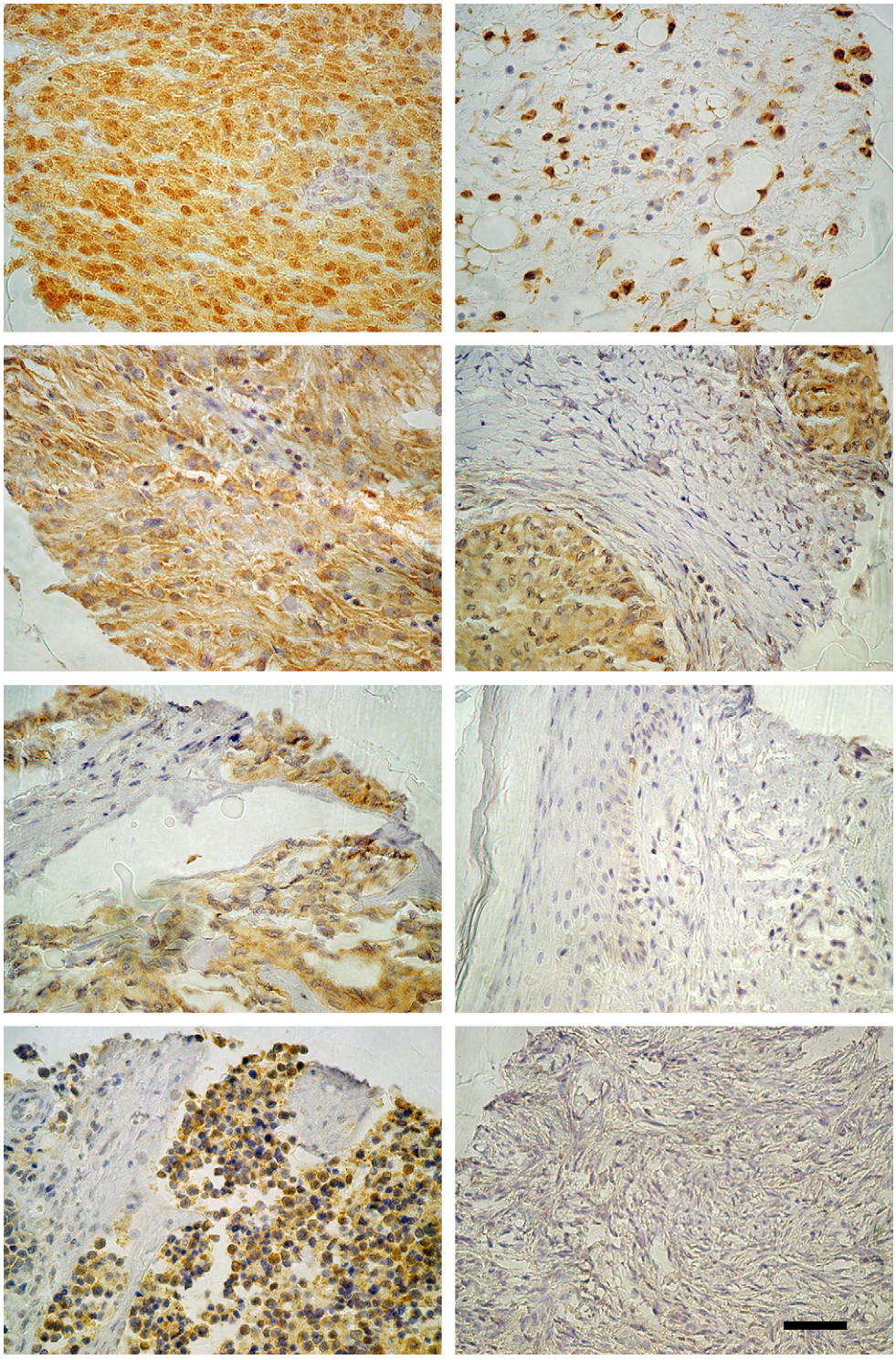

Figure 1 – ALG-2 is highly expressed in various cancers. Panel of tissue samples from the MTA. From top (left hand panel); Gastrointestinal tumors (GIST), malignant melanoma, synovial sarcoma, pancreatic neuroendocrine tumor (PNET) (right hand panel); liposarcoma, Brenner tumor, normal skin, normal ovary. Scale bar represents 50 μM.

and from normal tissue included as controls on the MTA. No ALG-2 staining was observed in stromal areas of normal tissue. Expression of ALG-2 was found in extranodal lymphocytes of all organs. Nodal lymphoid cells as well as lymphocytes of the spleen, thymus, and tonsils exhibited similar intensities of ALG-2 staining. Overall, cells of epithelial origin showed most significant staining intensities. Among cell types with highest ALG-2 expression were urothelial cells of both the

Table 1 – Individual tissue categories ranked according to the weighted sum of ALG-2 expression levels

Tissue category (individual tumors)	N	Weak (%)	Moderate (%)	Strong (%)	Positive (%)	Weighted sum	Rank
Ovary, Brenner tumor	9	11.1	11.1	55.6	77.8	66.7	1
Carcinoid tumor	45	22.2	33.3	33.3	88.8	62.9	2
Breast, cribriform cancer	8	12.5	37.5	25	75	54.2	3
PNET	15	60	20	20	100	53.3	4
Ovary, serous cancer	47	31.9	25.5	25.5	82.9	53.1	5
Kidney, chromophobic cancer	14	21.4	57.1	7.1	85.6	52.3	6
Small intestine, adenocarcinoma	11	27.3	36.4	18.2	81.9	51.6	7
Colon adenoma, mild dysplasia	45	35.6	31.1	17.8	84.5	50.4	8
Colon adenoma, moderate dysplasia	45	28.9	37.8	13.3	80	48.1	9
GIST	31	35.5	19.4	22.6	77.5	47.4	10
Colon adenoma, severe dysplasia	37	37.8	21.6	18.9	78.3	45.9	11
Thyroid, adenoma	46	43.5	26.1	13	82.6	44.9	12
Thymoma	23	34.8	30.4	13	78.2	44.9	13
Skin, malignant melanoma	47	36.2	29.8	12.8	78.8	44.7	14
Glioblastoma multiforme	47	36.2	29.8	12.8	78.8	44.7	15
Adrenal gland, adenoma	15	46.7	33.3	6.7	86.7	44.5	16
Skin, benign appendix tumor	31	29	35.5	9.7	74.2	43	17
Urinary bladder cancer, TCC non-invasive (pTa)	38	15.8	44.7	7.9	68.4	43	18
Colon, adenocarcinoma	39	35.9	23.1	15.4	74.4	42.8	19

Tissue categories with $N < 5$ have been excluded.

urinary bladder and the kidney pelvis. Also, islet cells of the pancreas, columnar cells of seminal vesicles and epididymis as well as ciliated and secretory cells of the fallopian tube showed high ALG-2 expression (Table 3). Tissues of mesenchymal origin did not show any detectable ALG-2 staining. None of the tissue samples on the NTA showed strong ALG-2 staining.

2.4. *Downregulation of ALG-2 leads to reduced viability*

In order to investigate whether ALG-2 may contribute to tumor cell viability we downregulated ALG-2 levels in HeLa cells and monitored the growth of these cells by assaying ATP levels following siRNA transfections. The cells were transfected with either two different siRNAs targeting ALG-2 or a previously described control sequence directed against luciferase (Elbashir et al., 2001). ALG-2 levels were efficiently downregulated following transfection with the ALG-2 siRNAs, whereas control transfected cells showed no changes in ALG-2 levels compared to non-transfected cells (Figure 3A). We observed that HeLa cells grew significantly slower following transfection with ALG-2 siRNAs as compared to control siRNA transfected cells (Figure 3B). Furthermore, HeLa cells with low ALG-2 levels were irregularly shaped (Figure 4A). Based on the

Table 2 – All neoplastic tissue categories ranked according to moderate plus strong expression levels of ALG-2

	N	Weak (%)	Moderate (%)	Strong (%)	Moderate/strong (%)	Rank
Urothelium, benign	39	15.4	43.6	7.7	51.3	1
Adeno dysplasia	127	33.9	30.7	16.5	47.2	2
Thymoma	23	34.8	30.4	13.0	43.5	3
Neuroendocrine	112	38.4	21.4	20.5	42.0	4
Undiff carcinoma	118	28.0	23.7	11.0	34.7	5
Melanocytic	89	36.0	23.6	10.1	33.7	6
Brain	159	44.0	27.0	6.3	33.3	7
Biphasic tumors	10	0.0	20.0	10.0	30.0	8
Adenoma	185	43.2	23.8	5.4	29.2	9
Adenocarcinoma	941	33.2	17.9	7.3	25.2	10
Sarcoma	200	30.0	13.5	7.0	20.5	11
Urothelium malignant	43	34.9	9.3	7.0	16.3	12
Hematologic	138	25.4	13.0	2.2	15.2	13
Undifferentiated	36	22.2	8.3	5.6	13.9	14
SQCC	400	19.3	7.0	2.5	9.5	15
Mesothelial	28	7.1	7.1	0.0	7.1	16
Germ cell	104	37.5	2.9	1.0	3.8	17
Mesenchymal benign	227	6.2	1.3	0.4	1.8	18
SQCC dysplasia	18	5.6	0.0	0.0	0.0	19
Total	3191	29.1	15.6	6.3	21.9	

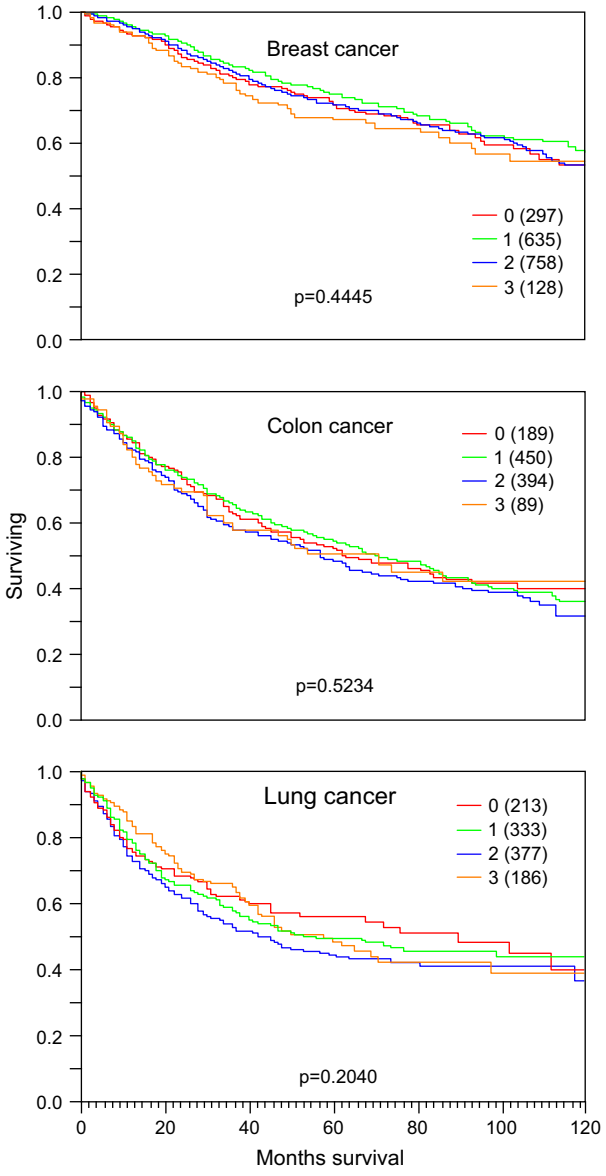

Figure 2 – ALG-2 levels were unrelated to patient survival in breast, colon, and lung cancers. Curves show the ratio of patient survival as a function of time of survival. ALG-2 staining intensities are indicated by colors: red (0, no staining), green (1, weak staining), blue (2, moderate staining), and orange (3, strong staining). Numbers in brackets indicate study group size.

morphology of the ALG-2 deficient cells (Figure 4A) and the observations that more floating cells were present in ALG-2 knockdown cultures than control cultures (not shown), we speculated that ALG-2 knockdown leads to increased cell death thereby contributing to the decreased growth rate. This was supported by FACS analysis showing an elevated number of dead cells in the HeLa cultures with downregulated ALG-2 levels compared to cells that were transfected with the control siRNA (Figure 4B). However, more experiments are needed to pinpoint the mode of cell death induced by ALG-2 downregulation.

3. Discussion

The recent finding that ALG-2 is upregulated in lung cancers and hepatomas (la Cour et al., 2003) led us to investigate ALG-2 expression in various neoplastic tissues and further to assess whether our anti-ALG-2 antibody can be used as a marker in cancer prognostics. In an attempt to find out whether ALG-2 may contribute to cancer cell viability we have analysed the effect of ALG-2 downregulation in HeLa cells. In this study we analysed the expression pattern of ALG-2 in 8120 tissue samples for, thus providing a comprehensive catalogue of ALG-2 expression in human normal tissues and cancers. In combination with functional analysis these data may indicate that ALG-2 is important for maintenance of cellular viability. In previous studies, upregulation of ALG-2 was found in several cancers, including lung, suggesting a possible role of ALG-2 in tumor progression. The large number of samples analysed in our study allowed for a detailed picture of ALG-2 expression patterns. According to our findings, ALG-2 dysregulation includes both overexpression and loss of expression in a comparatively small (30–40%) fraction of tumors. Furthermore, we have used TMAs to determine cell type specific ALG-2 expression in 442 normal tissue samples. Also, 307 intact normal tissue samples are represented on the multitumor TMA. In normal tissue, detectable ALG-2 levels were found in cells of epithelioid origin, whereas expression of ALG-2 was almost absent in mesenchymal cells. Interestingly, high expression of ALG-2 was found in synovial sarcomas and leiomyosarcomas indicating a role for ALG-2 in processes that lead to transformation of mesenchymal cells.

Previously, we found that normal liver tissue exhibits little ALG-2 expression compared to malignant liver tissue (la Cour et al., 2003). The present tissue analysis confirms this finding comparing 14 normal liver samples with 47 samples of hepatocellular carcinomas. Whereas normal liver samples showed only weak staining, 23% of the hepatocellular carcinomas had moderate/strong staining intensities (Supplementary Table ST1). Eleven normal lung tissue samples were represented on the TMAs, nine samples on the NTA and two samples on the MTA. None of the normal lung tissue samples stained positive for ALG-2, whereas approximately 80% of lung tumors showed weak to strong staining consistent with our initial report of ALG-2 upregulation in lung cancers (la Cour et al., 2003). ALG-2 staining intensity among different subtypes of non-small cell lung cancers also fitted well with our initial report of ALG-2 expression being highest in adenocarcinomas followed by squamous carcinomas and with lowest expression in large cell carcinomas (Supplementary Table ST1). The lack of detectable ALG-2 staining in the majority of the normal tissue samples is the result of controlled staining reaction to enable differentiation between moderately and strongly stained samples. Western blot analysis of tissue extracts indicated that ALG-2 could be found in all analysed tissue samples (la Cour et al., 2003). In the initial report of ALG-2 expression in tissue we found by Western blot analysis that ALG-2 was most highly expressed in normal endometrium, spleen, and kidney of mice (la Cour et al., 2003). These results were confirmed by the present analysis of ALG-2 expression in normal cells of human tissue.

Table 3 – Summary of the most intensely ALG-2 stained cell types from the normal tissue arrays

Organ	Cell type
Ovary	Stroma (spindle-shaped cell)+, granulosa cell of follicular cyst +
Kidney pelvis, urinary bladder	Urothelium++
Lymph node	Lymphoid cells (incl blasts)+
Spleen	Lymphocytes+
Thymus	Thymocyte (small lymphocyte)+
Tonsil	Lymphoid cells (incl blasts)+
All organs	Extranodal lymphocyte+, plasma cell+
Intestine (colon and small intestine)	Absorptive cell+, goblet cell+
Gallbladder	Columnar cell+
Pancreas	Islet cell++
Parotid gland	Columnar ductal cell+
Submandibullary gland	Columnar ductal cell+, serous cell+
Kidney, cortex	Connecting tubule cell+, intercalated cell+, principal cell+
Prostate	Columnar secretory cell+
Seminal vesicle	Columnar ductal cell++
Epididymis	Tall columnar cell++

The initial finding that ALG-2 functions as a proapoptotic protein (Vito et al., 1996) could not be confirmed by studies on T-cells isolated from ALG-2 knockout mice (Jang et al., 2002). In lack of clear functional evidence from ALG-2 knockout studies it is relevant to consider ALG-2 interaction partners for speculations of possible ALG-2 functions in survival pathways. A number of ALG-2 targets have been identified including AIP1/Alix, ASK1, HEED, annexin 7 (reviewed in Tarabykina et al., 2004) and more recently Raf-1 (Chen and Sytkowski, 2005), Tsg101 (Katoh et al., 2005), copines (Tomsig et al., 2003), HEBP2, c14orf32 (Rual et al., 2005), Sec 31A (la Cour et al., 2007; Shibata et al., 2007; Yamasaki et al., 2006 and Scotin (Draeby et al., 2007)). AIP1/Alix, which was identified as an ALG-2 target independently by two groups (Missotten et al., 1999; Vito et al., 1999), stands out as it has been shown in several systems to play a role in apoptosis together with ALG-2. AIP1/Alix was recently found to be involved in neuronal cell death, as overexpression led to caspase activation (Mahul-Mellier et al., 2006; Trioulier et al., 2004). Furthermore, overexpression of the C-terminus of AIP1/Alix containing the ALG-2 binding domain led to inhibition of caspase activation (Mahul-Mellier et al., 2006). These findings are compatible with an earlier investigation showing that a cell death protective phenotype inferred by overexpression of C-terminal AIP1/Alix could be annulled by co-overexpression of ALG-2 (Vito et al., 1999). Whether overexpression of ALG-2 alone leads to apoptosis is not known so far. Support for ALG-2 as a proapoptotic protein comes from recent work of Mahul-Mellier et al. (2006) who found in congruence with previous reports (Chatellard-Causse et al., 2002; Vito et al., 1999) that the part of AIP1/Alix shown to interact with ALG-2 is required for AIP1/Alix-induced cell death. Here we show for the first time that downregulation of ALG-2 in a human cancer cell line impairs viability.

Tsg101 is an example of an ALG-2 binding protein (Katoh et al., 2005) with dual seemingly opposing activities. On one hand Tsg101 has been described as an inhibitor of transformation of NIH3T3 fibroblasts (Li and Cohen, 1996) and on the other hand as an inhibitor of p53 independent cell cycle arrest and cell death in mouse embryonic fibroblasts (Krempler et al., 2002). It is therefore well possible that ALG-2, depending on the cellular context, may act as a cell death promoting protein or as cell viability factor acting even through the same effector protein.

Our findings that ALG-2 expression is higher in cells with endocrine functions as compared to non-endocrine cells can be interpreted with a role of ALG-2 in the secretion process. Indeed, this possibility is given by the fact that ALG-2 interacts with a component of the ER to Golgi vesicle transport apparatus, Sec31A, and affects its localization (la Cour et al., 2007; Shibata et al., 2007; Yamasaki et al., 2006). Enhanced expression of ALG-2 might therefore aid in supporting the increased protein production in cancer cells and thereby also protect from ER overload known to tamper with cell viability.

Our work provides a comprehensive overview on ALG-2 expression in normal and cancer tissues and gives evidence that this protein may work as a cell viability factor unrecognized in earlier work. Elucidation of the molecular mechanisms supporting a function of ALG-2 in cell viability will be in the center of future work.

4. Experimental procedures

4.1. *TMA construction*

TMA construction was as described by Kononen et al. (1998) and Schraml et al. (1999). Five different TMA sets were utilized for this study. The first was a multitumor array (MTA) including 3191 samples from 127 different primary tumor types and 307 control samples from various normal tissues. These samples are distributed among seven TMA blocks, each containing 400–500 tumors. To show the integrity of the array an example of a hematoxylin–eosin stained array section is given in Supplementary Figure SF1.

Three different TMAs with prognostic data were analysed, representing 1911 breast cancers (all with survival information), 1154 lung cancers (1125 with clinical follow up data), and 1116 colon cancers (1113 with survival information).

Analysis of ALG-2 expression in normal tissue was performed using a NTA constructed from 608 samples of 76 different normal tissue types falling into one of the three categories: mesenchymal tissues, surfaces, and solid organs. The

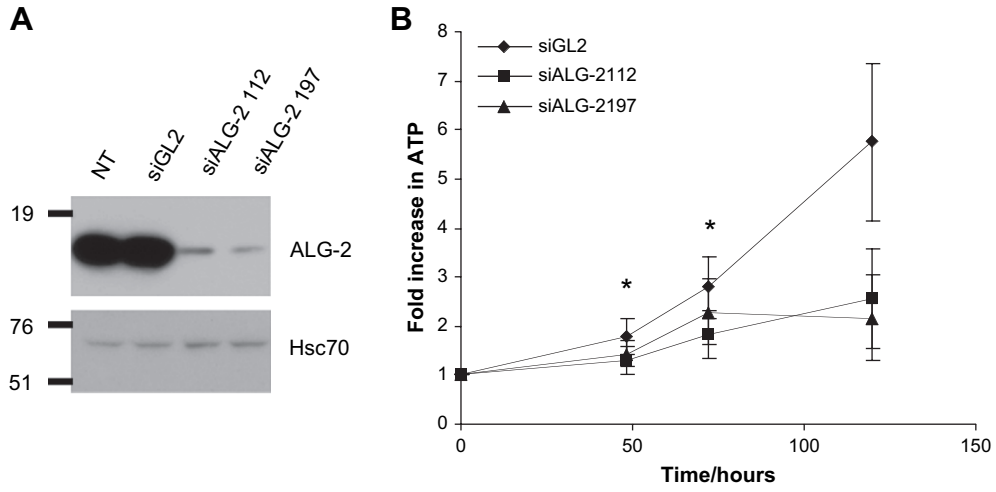

Figure 3 – ALG-2 knockdown leads to reduced cell growth (A): ALG-2 Western blot of HeLa cell lysates from non-transfected cells (NT) and from cells transfected with control siRNA (siGL2) or ALG-2 siRNAs (siALG-2 112 and siALG-2 197). Membranes were reprobed with anti-Hsc70 to confirm equal loading of lysates. (B): The increase in ATP content of HeLa cells following transfections with indicated siRNAs is shown as a function of time. Error bars represent the standard error of the mean (SEM) of three independent experiments and asterisks indicate $p < 0.04$ as determined by the paired *t*-test.

examined mesenchymal tissue types included aorta/intima, aorta/media, heart muscle, skeletal muscle, skeletal muscle of the tongue, myometrium, muscular walls of various organs (appendix, esophagus, stomach, ileum, colon descendens, kidney pelvis, and urinary bladder), penis (glans/corpus spongiosum), ovary (stroma), and fat tissue. The surface tissue punches included skin (surface, hairs, and sebaceous glands), lip, oral cavity, tonsil (surface epithelium), anal canal (skin and transitional epithelium), ectocervix, esophagus, kidney pelvis, urinary bladder, amnion/chorion, stomach (antrum and corpus), small intestine (duodenum and ileum), appendix, colon descendens, rectum, gallbladder, bronchus, and paranasal sinus. The solid organs included lymph node, spleen, thymus, tonsil, liver, pancreas, parotid gland, submandibullary gland, sublingual gland, small salivary glands of the lip, duodenum (Brunner gland), kidney cortex, kidney medulla, prostate, seminal vesicle, epididymis, testis, lung (parenchyma and bronchial glands), breast, endocervix, endometrium (proliferation, secretion, and early decidua), fallopian tube, placenta (first trimenon and mature), ovary (stroma, corpus luteum, and follicular cyst), adrenal gland, parathyroid gland, thyroid, cerebellum, cerebrum and pituitary gland (posterior lobe and anterior lobe) .

In cases where tissue intact original data files containing histological staining profiles of all tissue microarrays and prognostic data are available by contacting the corresponding author.

4.2. *Immunohistochemistry*

All immunohistochemical analyses were performed using a polyclonal antibody directed against ALG-2 as previously described (la Cour et al., 2003) In brief, immunostaining was performed following deparaffinizing and antigen retrieval by microwave heating in an alkaline Tris buffer. Endogenous peroxidase activity was quenched by hydrogen peroxide and slides were blocked for 1 h followed by overnight incubation with 4 μg/ml of anti-ALG-2 antibody. Detection was performed using the EnVision+ secondary antibody system followed by the peroxidase chromogen substrate, DAB+, both from Dako (Dako, Glostrup, Denmark).

For each tumor sample the staining intensity was judged as negative (no staining), + (weak), ++ (moderate), or +++ (strong staining).

4.3. *TMA Statistics*

Contingency table analysis and Chi-square tests were used to study the relationship between the level of ALG-2 expression and clinico-pathological parameters. Log rank tests were applied to estimate the impact of ALG-2 expression on patient prognosis.

4.4. *Cell cultures and siRNA transfections*

HeLa cells were grown in DMEM medium supplemented with 10% fetal bovine serum and 1% penicillin/streptomycin. The cells were cultured at 37 °C in a humidified incubator with 5% CO_2. The day prior to siRNA transfection HeLa cells (7800 cells/cm^2) were seeded. Transfections were performed using Oligofectamine reagent according to the manufacturer's transfection protocol (Invitrogen, Carlsbad, CA). The final concentration of ALG-2 siRNA used was 50 nM. Cells used for the viability assay were transfected twice. Thus, HeLa cells were transfected in culture flasks and replated in 96 well plates the day after transfection. Two siRNA duplex oligonucleotides against the ALG-2 gene (siALG-2) were used for targeting positions 112–130 and 197–215 downstream of the start codon ATG of the human ALG-2 gene (GenBank accession no. NM_013232). (ALG-2 112 sense RNA: 5′-GACAGGAGUGGAGUGAUAUdTdT-3′; ALG-2 112 antisense RNA: 5′-AUAUCACUCCACUCCUGU CdTdT-3′. ALG-2 197 sense RNA: 5′-GGUCGAUCAUAUCCAUGU UdTdT-3′; ALG-2 197 antisense RNA: 5′-AACAUGGAUAUGAUC

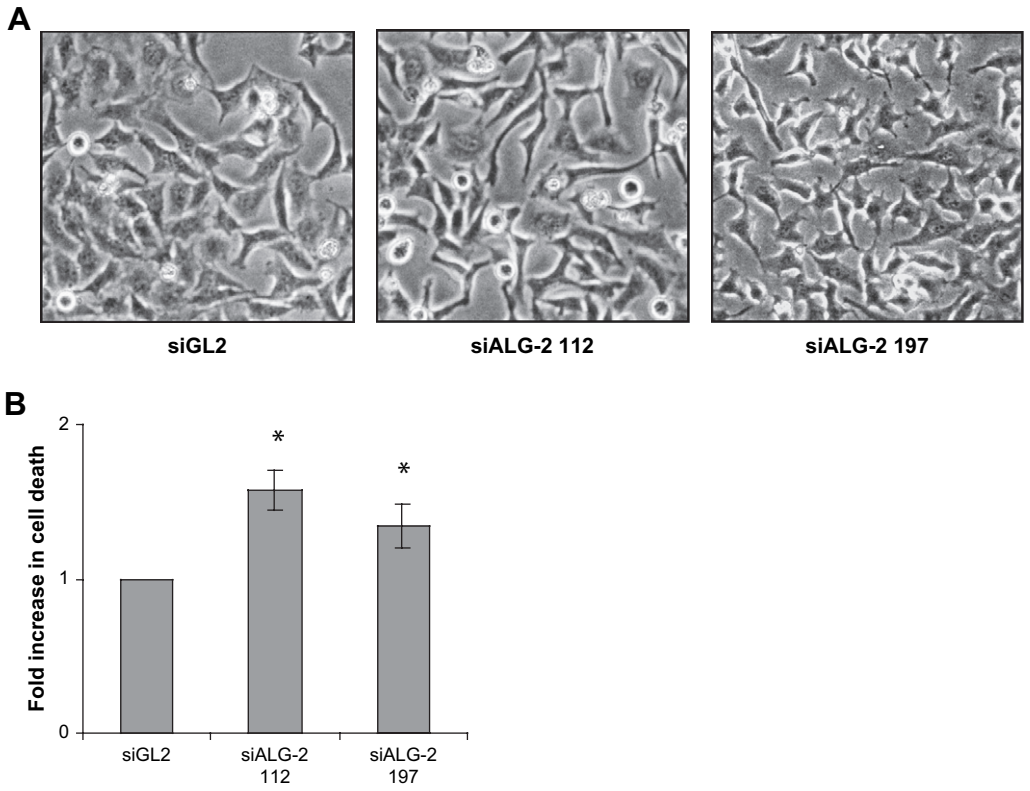

Figure 4 – ALG-2 knockdown leads to morphological changes and cell death. (A): phase contrast micrographs of HeLa cell cultures 72 h after transfection with control sequence (siGL2) or siALG-2 sequences. (B): Cell death as measured by cell permeability to 7-AAD in HeLa cells 3 days after transfection. Error bars represent the SEM of three independent experiments and asterisks indicate $p < 0.04$ as determined by the paired *t*-test.

GACCdTdT-3′). Control cells were transfected with siRNA duplex oligonucleotides against the firefly luciferase gene (siGL2) (GL2 sense RNA: 5′-CGUACGCGGAAUACUUCGAdTdT-3′; GL2 antisense RNA: 5′-UCGAAGUAUUCCGCGUACGdTdT-3′). All siRNA duplex oligonucleotides were from Dharmacon (Dharmacon, Lafayette, CO).

4.5. *Western blot analysis*

Lysates of HeLa cells isolated three days after siRNA transfection were prepared in lysis buffer (0.5% NP40, 50 mM Tris pH 7.4, 150 mM NaCl) containing 1:1000 dilution of a cocktail of protease inhibitors (Sigma–Aldrich, St. Louis, MO). The lysates were centrifuged at 15,000 × *g* for 10 min at 4 °C and protein content in the supernatant was quantified using the Bio-Rad DC Protein Assay (Bio-Rad Laboratories, Hercules, CA). Sample buffer (0.25 M Tris pH 8.8, 10% sodium dodecyl sulfate (SDS), 0.5% bromphenol blue, 0.1 M dithiothreitol (DTT), 0.5 M sucrose) was added to protein extracts and the proteins were separated by 10% SDS-polyacrylamide gel electrophoresis (SDS-PAGE) and transferred to polyvinyl difluoride (PVDF) membranes, Hybond-P (Amersham Biosciences, Uppsala, Sweden). Western blot analyses were performed using a polyclonal anti-ALG-2 antibody as previously described (la Cour et al., 2003) Anti-Hsc70 antibody (Santa Cruz Biotechnology, Santa Cruz, CA, USA) was used as a loading control.

4.6. *Viability assay*

Cells seeded in 96 well plates were harvested at different time points after siRNA transfection and lysed in ATP determination lysis buffer (10 mM NaH_2PO_4, 10 mM Na_2HPO_4, 150 mM NaCl, 1 mM DTT, 2 mM ethylenediaminetetraacetic acid, 1% Triton X-100). ATP content was determined by chemiluminescence exploiting the ATP dependent oxidation of D-luciferin by luciferase. The reagents for the ATP assay were supplied by Invitrogen and measurements were performed in 96 well plates according to the manufacturer's instructions (Invitrogen, Carlsbad, CA) using a Wallac Victor plate reader (Perkin–Elmer, Waltham, MA).

4.7. *Cell death assay*

Cell death was measured 3 days after a single siRNA transfection. Both detached and attached cells were collected. The attached cells were harvested by a brief trypsin treatment. Cells were washed once in phosphate buffered saline (10 mM NaH_2PO_4, 10 mM Na_2HPO_4, 150 mM NaCl) and resuspended to 1×10^6 cells/ml in a buffer containing 0.01 M HEPES, pH 7.4; 0.14 M NaCl; 0.25 mM $CaCl_2$. Cells were incubated at room temperature for 15 min in a buffer containing 8 μg/ml 7-amino-actinomycin D (7-AAD, Sigma–Aldrich). Samples were kept in dark on ice until analysed using flow cytometry (FACScan, BD Biosciences, Franklin Lakes, NJ).

Acknowledgements

This work was supported by funds from The Danish Research Council, The Danish Cancer Society and The Lundbeck Foundation. Svetlana Tarabykina is acknowledged for critical reading of the manuscript.

Appendix A. Supplementary data

Supplementary data associated with this article can be found, in the online version, at doi:10.1016/j.molonc.2007.08.002.

REFERENCES

Chatellard-Causse, C., Blot, B., Cristina, N., Torch, S., Missotten, M., Sadoul, R., 2002. Alix (ALG-2-interacting protein X), a protein involved in apoptosis, binds to endophilins and induces cytoplasmic vacuolization. J. Biol. Chem. 277, 29108–29115.

Chen, C., Sytkowski, A.J., 2005. Apoptosis-linked gene-2 connects the Raf-1 and ASK1 signalings. Biochem. Biophys. Res. Commun. 333, 51–57.

la Cour, J.M., Mollerup, J., Berchtold, M.W., 2007. ALG-2 oscillates in subcellular localization, unitemporally with calcium oscillations. Biochem. Biophys. Res. Commun. 353, 1063–1067.

la Cour, J.M., Mollerup, J., Winding, P., Tarabykina, S., Sehested, M., Berchtold, M.W., 2003. Up-regulation of ALG-2 in hepatomas and lung cancer tissue. Am. J. Pathol. 163, 81–89.

Draeby, I., Woods, Y.L., la Cour, J.M., Mollerup, J., Bourdon, J.C., Berchtold, M.W., 2007. The calcium binding protein ALG-2 binds and stabilizes Scotin, a p53-inducible gene product localized at the endoplasmic reticulum membrane. Arch. Biochem. Biophys. 467, 87–94.

Elbashir, S.M., Harborth, J., Lendeckel, W., Yalcin, A., Weber, K., Tuschl, T., 2001. Duplexes of 21-nucleotide RNAs mediate RNA interference in cultured mammalian cells. Nature 411, 494–498.

Jang, I.K., Hu, R., Lacana, E., D'Adamio, L., Gu, H., 2002. Apoptosis-linked gene 2-deficient mice exhibit normal T-cell development and function. Mol. Cell Biol. 22, 4094–4100.

Katoh, K., Suzuki, H., Terasawa, Y., Mizuno, T., Yasuda, J., Shibata, H., Maki, M., 2005. The penta-EF-hand protein ALG-2 interacts directly with the ESCRT-I component TSG101, and Ca2+-dependently co-localizes to aberrant endosomes with dominant-negative AAA ATPase SKD1/Vps4B. Biochem. J. 391, 677–685.

Kononen, J., Bubendorf, L., Kallioniemi, A., Barlund, M., Schraml, P., Leighton, S., Torhorst, J., Mihatsch, M.J., Sauter, G., Kallioniemi, O.P., 1998. Tissue microarrays for high-throughput molecular profiling of tumor specimens. Nat. Med. 4, 844–847.

Krempler, A., Henry, M.D., Triplett, A.A., Wagner, K.U., 2002. Targeted deletion of the Tsg101 gene results in cell cycle arrest at G1/S and p53-independent cell death. J. Biol. Chem. 277, 43216–43223.

Li, L., Cohen, S.N., 1996. Tsg101: a novel tumor susceptibility gene isolated by controlled homozygous functional knockout of allelic loci in mammalian cells. Cell 85, 319–329.

Mahul-Mellier, A.L., Hemming, F.J., Blot, B., Fraboulet, S., Sadoul, R., 2006. Alix, making a link between apoptosis-linked gene-2, the endosomal sorting complexes required for transport, and neuronal death in vivo. J. Neurosci. 26, 542–549.

Maki, M., Narayana, S.V., Hitomi, K., 1997. A growing family of the Ca2+-binding proteins with five EF-hand motifs. Biochem. J. 328 (Pt 2), 718–720.

Matsuo, H., Chevallier, J., Mayran, N., Le Blanc, I., Ferguson, C., Faure, J., Blanc, N.S., Matile, S., Dubochet, J., Sadoul, R., et al., 2004. Role of LBPA and Alix in multivesicular liposome formation and endosome organization. Science 303, 531–534.

Missotten, M., Nichols, A., Rieger, K., Sadoul, R., 1999. Alix, a novel mouse protein undergoing calcium-dependent interaction with the apoptosis-linked-gene 2 (ALG-2) protein. Cell Death Differ. 6, 124–129.

Mollerup, J., Krogh, T.N., Nielsen, P.F., Berchtold, M.W., 2003. Properties of the co-chaperone protein p23 erroneously attributed to ALG-2 (apoptosis-linked gene 2). FEBS Lett. 555, 478–482.

Odorizzi, G., 2006. The multiple personalities of Alix. J. Cell Sci. 119, 3025–3032.

Rual, J.F., Venkatesan, K., Hao, T., Hirozane-Kishikawa, T., Dricot, A., Li, N., Berriz, G.F., Gibbons, F.D., Dreze, M., Ayivi-Guedehoussou, N., et al., 2005. Towards a proteome-scale map of the human protein–protein interaction network. Nature 437, 1173–1178.

Schraml, P., Kononen, J., Bubendorf, L., Moch, H., Bissig, H., Nocito, A., Mihatsch, M.J., Kallioniemi, O.P., Sauter, G., 1999. Tissue microarrays for gene amplification surveys in many different tumor types. Clin. Cancer Res. 5, 1966–1975.

Shibata, H., Suzuki, H., Yoshida, H., Maki, M., 2007. ALG-2 directly binds Sec31A and localizes at endoplasmic reticulum exit sites in a Ca2+-dependent manner. Biochem. Biophys. Res. Commun. 353, 756–763.

Sperandio, S., Poksay, K., de Belle, I., Lafuente, M.J., Liu, B., Nasir, J., Bredesen, D.E., 2004. Paraptosis: mediation by MAP kinases and inhibition by AIP-1/Alix. Cell Death Differ. 11, 1066–1075.

Strack, B., Calistri, A., Craig, S., Popova, E., Gottlinger, H.G., 2003. AIP1/ALIX is a binding partner for HIV-1 p6 and EIAV p9 functioning in virus budding. Cell 114, 689–699.

von Schwedler, U.K., Stuchell, M., Muller, B., Ward, D.M., Chung, H.Y., Morita, E., Wang, H.E., Davis, T., He, G.P., Cimbora, D.M., et al., 2003. The protein network of HIV budding. Cell 114, 701–713.

Tarabykina, S., Moller, A.L., Durussel, I., Cox, J., Berchtold, M.W., 2000. Two forms of the apoptosis-linked protein ALG-2 with different Ca(2+) affinities and target recognition. J. Biol. Chem. 275, 10514–10518.

Tarabykina, S., Mollerup, J., Winding, P., Berchtold, M.W., 2004. ALG-2, a multifunctional calcium binding protein? Front. Biosci. 9, 1817–1832.

Tomsig, J.L., Snyder, S.L., Creutz, C.E., 2003. Identification of targets for calcium signaling through the copine family of proteins. Characterization of a coiled-coil copine-binding motif. J. Biol. Chem. 278, 10048–10054.

Trioulier, Y., Torch, S., Blot, B., Cristina, N., Chatellard-Causse, C., Verna, J.M., Sadoul, R., 2004. Alix, a protein regulating endosomal trafficking, is involved in neuronal death. J. Biol. Chem. 279, 2046–2052.

Vito, P., Lacana, E., D'Adamio, L., 1996. Interfering with apoptosis: Ca(2+)-binding protein ALG-2 and Alzheimer's disease gene ALG-3. Science 271, 521–525.

Vito, P., Pellegrini, L., Guiet, C., D'Adamio, L., 1999. Cloning of AIP1, a novel protein that associates with the apoptosis-linked gene ALG-2 in a Ca2+-dependent reaction. J. Biol. Chem. 274, 1533–1540.

Wu, Y., Pan, S., Luo, W., Lin, S.H., Kuang, J., 2002. Hp95 promotes anoikis and inhibits tumorigenicity of HeLa cells. Oncogene 21, 6801–6808.

Yamasaki, A., Tani, K., Yamamoto, A., Kitamura, N., Komada, M., 2006. The Ca2+-binding Protein ALG-2 is recruited to endoplasmic reticulum exit sites by Sec31A and stabilizes the localization of Sec31A. Mol. Biol. Cell 17, 4876–4887.